Institute of Physics Publishing — Semiconductor Science and Technology
Semicond. Sci. Technol. **21** (2006) 822–828 doi:10.1088/0268-1242/21/6/021

Determination of the characteristic parameters of Sn/n-GaAs/Al–Ge Schottky diodes by a barrier height inhomogeneity model

H Doğan[1], N Yıldırım[1], A Turut[1], M Biber[1], E Ayyıldız[2] and Ç Nuhoğlu[1]

[1] Department of Physics, Faculty of Sciences and Arts, Atatürk University, 25240 Erzurum, Turkey
[2] Department of Physics, Faculty of Sciences and Arts, Erciyes University, Kayseri, Turkey

Received 24 February 2006, in final form 5 April 2006
Published 9 May 2006
Online at stacks.iop.org/SST/21/822

Abstract
A study on parameters of the Sn/n-GaAs Schottky barrier diode (SBD) fabricated on an n-type GaAs substrate has been made. The Sn/n-GaAs SBD has shown a nearly ideal behaviour with ideality factor and barrier height (BH) values of 1.081 and 0.642 eV, respectively, from the experimental forward-bias current–voltage (*I–V*) characteristics. A BH value of 0.724 eV has been obtained from the experimental reverse-bias capacitance–voltage (*C–V*) characteristics. An accurate theoretical modelling of the effect of the presence of inhomogeneities on the electron transport across the metal–semiconductor interface has been applied. This model attempts to explain abnormal experimental results obtained on 'real' Schottky diodes. Our results clearly demonstrate that the electron transport at the metal–semiconductor interface is significantly affected by low-barrier regions (patches). When the experimental data are described by the thermionic emission theory of inhomogeneous Schottky contacts, it has been concluded that both the experimental forward and reverse *I–V* characteristics and the difference between the values of the experimental *I–V* and *C–V* SBHs should be considered. An experimental BH difference of $\Delta = 0.082$ V has been obtained for the Sn/n-GaAs SBD that is less than the critical value; therefore, it has been seen that the potential in front of the patch is not pinched off.

1. Introduction

The formation of the Schottky barrier at the metal–semiconductor (MS) interface has been a subject of extensive investigations for several years and a full understanding of the nature of their electrical characteristics is of great interest [1–7]. It is well known that interface properties of the MS contacts have a dominant influence on the device performance, reliability and stability [5–14]. Schottky barrier inhomogeneity at MS interfaces has been considered as an important factor in explaining the non-ideal behaviour of the Schottky diodes and the dependence of the Schottky barrier (SB) values on the doping level and measurement methods used [8–19]. Ballistic electron emission microscopy (BEEM) has also supported the existence of Gaussian distribution of barrier heights (BHs) in Schottky diodes [20–23].

Some experimental and theoretical works, however, have revealed that the physics of Schottky barrier height (SBH) formation is determined by the interface structure on a nanometre-scale length [22–28]. An accurate theoretical modelling of the effect of such inhomogeneities on the electron transport across the metal–semiconductor (MS) interface was quantitatively developed by Sullivan *et al* [24] and Tung [25, 26], taking into account the possible presence of specific distribution of nanometre-scale interfacial 'patches' (small regions) with lower barrier height embedded in an interface with an otherwise uniform high barrier. This model [24–26] gives an explanation for a large series of abnormal experimental results on 'real' Schottky contacts, such as ideality factors greater than unity, temperature dependence of the Schottky barrier height (SBH) and ideality factor, soft reverse characteristics and the strong correlation that is often observed between the SBH and the ideality factor measured on sets of diodes as mentioned in [27–31].

The purpose of this paper is to investigate, according to the model of Sullivan [24] and Tung [25], the experimental forward- and reverse-bias *I–V* characteristics of the nearly ideal Sn/n-GaAs Schottky diodes fabricated from the chemically cleaned n-type GaAs surface. An accurate theoretical modelling of the effect of the presence of inhomogeneities on the electron transport across the metal–semiconductor interface is applied with the assumption of a statistical distribution of the patch characteristics in this model [25].

2. Experimental procedure

The Sn/n-GaAs/Au–Ge Schottky diodes have been prepared using cleaned and polished n-GaAs (as received from the manufacturer) with [1 0 0] orientation and 2–5 × 10^{17} cm^{-3} carrier concentrations. Before making contacts, the n-GaAs wafer was dipped in $5H_2SO_4 + H_2O_2 + H_2O$ solution for 1.0 min to remove the surface damage layer and undesirable impurities and then in H_2O + HCl solution followed by a rinse in deionized water of 18 MΩ. The wafer has been dried with high-purity nitrogen and inserted into the deposition chamber immediately after the etching process. Au–Ge (88%, 12%) for Ohmic contacts was evaporated on the back of the wafer in a vacuum-coating unit of 10^{-5} Torr. Then, low resistance Ohmic contacts were formed by thermal annealing at 450 °C for 3 min in flowing N_2 in a quartz tube furnace. The Schottky contacts have been formed by evaporating Sn as dots with a diameter of about 1.35 mm on the front surface of n-GaAs. The current–voltage (*I–V*) and capacitance–voltage (*C–V*) characteristics have been measured using an HP 4140B picoampermeter and an HP model 4192A LF impedance analyser, respectively, at room temperature and in the dark.

3. Results and discussion

3.1. Capacitance–voltage (C–V) characteristics

Figure 1 shows the experimental reverse-bias C^{-2}–V curve of the Sn/n-GaAs SBD at 500 kHz and at room temperature. These *C–V* data are independent of frequency because the measurements are carried out at sufficiently high frequencies. Thus, in Schottky diodes, the depletion layer capacitance can be expressed as [32–34]

$$C^{-2} = 2(V_{d0} + V)/q\varepsilon_s A^2 N_d. \tag{1}$$

The slope of the reverse-bias C^{-2}–V plot can also be given by

$$\frac{d(C^{-2})}{dV} = \frac{2}{q\varepsilon_s A^2 N_d}, \tag{2}$$

where A is the area of the diode, V_{d0} is the diffusion potential at zero bias and is determined from the extrapolation of the linear C^{-2}–V plot to the V-axis. As can be seen from figure 1, a value of 0.684 V for intercept voltage of the sample, $V_{d0} = V_0$, was deduced, and thus a barrier height (BH) value of $\Phi_b^{CV} = 0.724$ eV, where $\Phi_b^{CV} = V_0 + V_n$, V_n is the potential difference between the Fermi level and the bottom of the conduction band for n-GaAs in the neutral region; it can be calculated knowing the carrier concentration N_d from the slope of the linear C^{-2}–V plot and is obtained from the following relation:

$$V_n = (kT)\ln\left(\frac{N_c}{N_d}\right), \tag{3}$$

where $N_c = 4.53 \times 10^{17}$ cm^{-3} is the state density in the valence band for n-GaAs [35], and an experimental value of $N_d = 2.53 \times 10^{17}$ cm^{-3} for the carrier concentration was calculated from the *C–V* characteristics in figure 1. The barrier height of $\Phi_b^{CV} = 0.724$ eV for the Sn/n-GaAs diode is in close agreement with the value of $\Phi_b^{IV} = 0.72$ eV for Sn/n-GaAs SBD ($N_d = 2 \times 10^{17}$ cm^{-3}) with $n = 1.12$ reported by Newman *et al* [36].

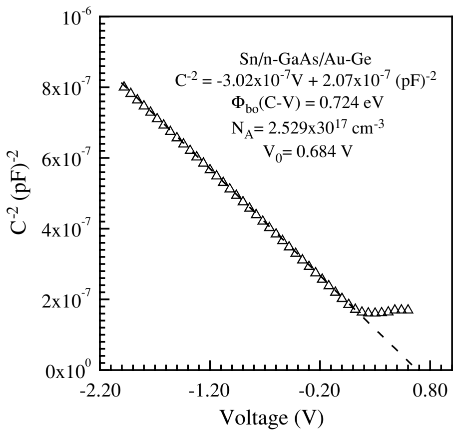

Figure 1. The reverse-bias C^{-2}–V curve of the Sn/n-GaAs Schottky diode at 500 kHz and room temperature.

3.2. Current–voltage (I–V) characteristics

When the Schottky barrier diodes (SBDs) are considered, it is assumed that the forward-bias current of the device is due to the thermionic emission current and it can be expressed as [33, 34]

$$I = I_0\left[\exp\left(\frac{qV - IR_s}{nkT}\right) - 1\right], \tag{4}$$

where

$$I_0 = AA^*T^2\exp\left(-\frac{q\Phi_{eff}}{kT}\right) \tag{5}$$

is the saturation current density, Φ_{eff} is the zero bias or effective barrier height, A^* is the effective Richardson constant and equals 8.16 A cm^{-2} K^{-2} for n-type GaAs, A is the diode area, R_s is the series resistance of the substrate and dominates in the higher bias region, n is an ideality factor and is a measure of conformity of the diode to pure thermionic emission and if n is equal to 1, pure thermionic emission occurs. However, n has usually a value greater than unity. It is obtained from the slope of the straight line region of the forward-bias

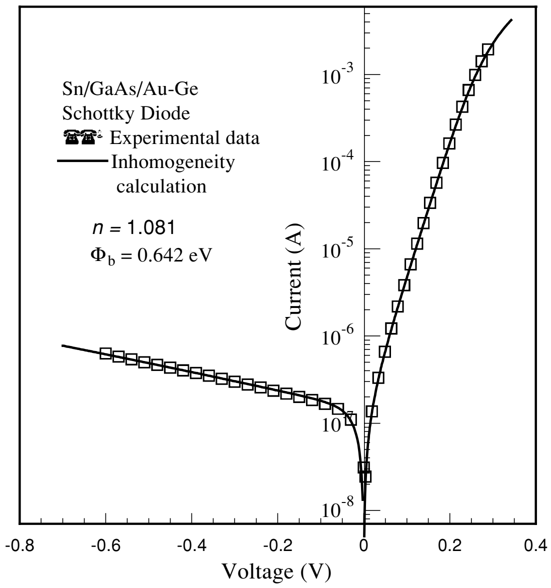

Figure 2. The forward- and reverse-bias current–voltage characteristics of the Sn/n-GaAs Schottky barrier diode at room temperature. The full line is a fit of equation (9) to the experimental data with $\Phi_{bo}^{hom} = 0.724$ eV, $R_s = 12\ \Omega$, $\sigma = 2.26 \times 10^{-5}$ cm$^{2/3}$ V$^{1/3}$ and $\rho = 1.12 \times 10^{12}$ cm^{-2}. The experimental data give an effective barrier height of 0.642 eV and an ideality factor of 1.081 using equations (5) and (6).

ln *I*–*V* characteristics through the relation

$$n = \frac{q}{kT}\frac{\mathrm{d}V}{\mathrm{d}(\ln I)}. \tag{6}$$

Figure 2 shows the experimental semilog forward- and reverse-bias *I*–*V* characteristics indicated by open squares of the Sn/n-GaAs Schottky contacts. An experimental barrier height value of 0.642 eV for the Sn/n-GaAs Schottky diode was calculated with the help of equation (5) from the *y*-axis intercepts of the semilog forward-bias *I*–*V* plots in figure 2, and an experimental value of 1.081 for *n* using equation (6). Moreover, the 'soft' or slight non-saturating behaviour observed as a function of bias in the experimental reverse-bias branch in figure 2 may be explained in terms of the spatial inhomogeneity of the Schottky barrier height (SBH) [24]. This bias dependence of the SBH is frequently observed experimentally; however, in many cases the observed voltage dependence of the barrier height determined from the reverse characteristics exceeds the expected result based on image-force lowering. The existence of SBH inhomogeneity offers a natural explanation for the soft reverse characteristics observed experimentally [24]. For inhomogeneous MS contacts, the reverse current may be dominated by the current which flows through the low-SBH patches, which is controlled by the potential at the saddle point. Increasing reverse bias drops the potential at the saddle point; hence, the reverse current increases with increasing reverse bias and does not saturate [24].

As has been seen, the C^{-2}–*V* curve gave the Schottky BH value higher than those derived from *I*–*V* measurements as expected. The reason for the discrepancy between the measured *I*–*V* and *C*–*V* SBH is clear. This difference is approximately 0.082 eV. Although the discrepancy could be explained by the existence of an excess capacitance at MS contacts due to an interfacial native oxide layer between the semiconductor and the Schottky contact metal, the existence of BH inhomogeneity offers another explanation. The difference between the measured *I*–*V* and *C*–*V* SBH in the metal/semiconductor is an evidence for Schottky BH inhomogeneity. The current in the *I*–*V* measurement is dominated by the current which flows through the region of low SBH. When the low-SBH patch is pinched off, the effective SBH of the patch is the potential at the saddle point. The measured *I*–*V* BH is significantly lower than the weighted arithmetic average of the SBHs. On the other hand, the *C*–*V* measured SBH is influenced by the distribution of charge at the depletion region boundary and this charge distribution follows the weighted arithmetic average of the SBH inhomogeneity; hence, the SBH determined by *C*–*V* is always close to the weighted arithmetic average of the SBHs in the inhomogeneous MS contact. The SBH determined from the zero bias intercept assuming thermionic emission as the current transport mechanism is below the measured *C*–*V* BH and the weighted arithmetic average of the SBHs [15, 24]. That is, we find $\Phi_b^{CV} = \bar{\Phi}_b$; the capacitance barrier Φ_b^{CV} is equal to the mean barrier $\bar{\Phi}_b$.

The downward curvature in the forward *I*–*V* plots at sufficiently large applied voltage is due to bulk series resistance of the GaAs substrate. The Φ_b, *n* and bulk series resistance values were also determined from the functions in [37–39] derived from equation (4):

$$\frac{\mathrm{d}V}{\mathrm{d}(\ln I)} = IR_s + n\frac{kT}{q}, \tag{7}$$

$$H(I) = V - n\frac{kT}{q}\ln\left(\frac{I}{AA^*T^2}\right) = IR_s + n\Phi_{\mathrm{eff}}. \tag{8}$$

Equation (7) should give a straight line for the data of downward curvature region of the forward-bias *I*–*V* characteristics. Thus, the slope and *y*-axis intercept of the $\mathrm{d}V/\mathrm{d}(\ln I)$ versus *I* plot will give R_s and nkT/q, respectively. The least-squares fits were used in drawing the curves related to R_s. The plots associated with these functions are given in figure 3. An *n* value of 1.083 was determined from equation (7). A plot of $H(I)$ versus *I* according to equation (8) will also give a straight line with the *y*-axis intercept equal to $n\Phi_b$. The slope of this plot also provides a second determination of R_s that can be used to check the consistency of Cheung's approach [38]. From equation (7) according to the $\mathrm{d}V/\mathrm{d}(\ln I)$ versus *I* plot, the values of 11.95 Ω and 1.081 for R_s and the ideality factor *n* of the device were obtained, respectively. The values of 11.39 Ω and 0.657 eV for R_s and Φ_b were also obtained from $H(I)$–I plots, respectively. As can be seen, the R_s values obtained from both plots are in close agreement with each other.

As seen from the above explanations [21–27], the inhomogeneities may play an important role and have to be considered in the evaluation of experimental *I*–*V* characteristics. The application of standard procedures (equation (4)) gives the effective BH and ideality factors only. To explain commonly observed deviations from the standard thermionic emission theory (TET) (all the 'anomalies' of the BH and ideality factor), Tung [25] has treated a system of discrete regions or low-barrier 'patches' embedded in a higher

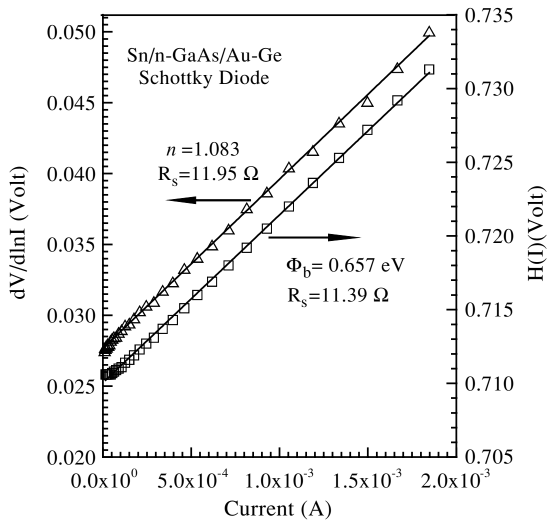

Figure 3. The experimental $dV/d(\ln I)$ versus I and $H(I)$ versus I plots for the pyronine-B/p-Si Schottky diode at room temperature. The slope and y-axis intercept of the $dV/d(\ln I)$ versus I plot give values of 1.081 and 11.95 Ω for R_s and n, respectively. The plot of $H(I)$ versus I gives values of 11.39 Ω and 0.657 eV for R_s and Φ_b, respectively.

uniform barrier. The nanometre-sized patches are taken to be small relative to the size of the depletion region such that the interaction of the patch with the surrounding depletion region causes a pinch-off or saddle point in the potential barrier away from the interface. For small and circular patches, assuming a Gaussian distribution of low-SBH circular patches characterized by a distribution of γ with standard deviation σ_T, Tung [25] gives the following form of the total current:

$$I = AA^*T^2 \exp\left(-\beta\ \Phi_{bo}^{hom}\right)[\exp(\beta(V - IR_S)) - 1](1 + P). \tag{9}$$

This also consists of $V \leqslant 3\ kT/q$ values. The other terms except for $(1 + P)$ on the right-hand side of equation (9) are the thermionic emission current of a homogeneous Schottky contact of area A, the series resistance R_s and homogeneous barrier height Φ_{bo}^{hom}; moreover, $\beta = q/kT$. The additional current term P is the patch function and depends on the area density, ρ, and strength factors, γ, of the patches. The strength parameter γ of a given patch is related to its radius R_p and decrease in barrier at the interface Δ_p (the local lowering of the BH at the saddle point in front of a circular patch of radius R_p) and is given by

$$\gamma = 3\left(\frac{R_p^2\Delta_p}{4}\right)^{1/3}. \tag{10}$$

Furthermore, if the strength parameter γ has a Gaussian distribution for $\gamma \geqslant 0$, the patch function P can be expressed as

$$P = \frac{8\pi\rho\sigma_T^2\eta^{1/3}}{9(V_{bo} - V + IR_s)^{1/3}} \exp\left(\frac{\beta^2\sigma_T^2(V_{bo} - V + IR_s)^{2/3}}{2\eta^{2/3}}\right), \tag{11}$$

where σ_T is the standard deviation of γ around zero and $\eta = \varepsilon_s\varepsilon_0/qN_d$, ε_s and N_d are the dielectric constant and the dopant density of the bulk semiconductor, respectively. V_{bo} is the interface band bending of the uniform barrier outside the patch and ρ is the patch density. Thus, equation (9) completely describes the current through inhomogeneous Schottky contacts that exhibit circular patches with a Gaussian distribution of the patch parameter γ and does not include the image-force lowering of the BH. Consequently, the current in equation (9) is made up of two compounds: one being the current over the entire diode which has a uniform SBH of Φ_{bo}^{hom} and an area A, the other being an additional current due to the presence of the low-SBH patches [25]. The combined effect of all the low-SBH regions is as if there were a big low-SBH region in the diode with an effective area of ρAA_{eff} and an effective SBH of [25]

$$\Phi_{eff} = \Phi_{bo}^{hom} - \Delta\Phi, \qquad \Delta\Phi = \frac{\sigma_T^2}{2kT}\left(\frac{V_{bo}}{\eta}\right)^{2/3}. \tag{12}$$

For a current described by equation (9), the ideality factor is given by [25]

$$n \approx 1 + \Delta n, \qquad \Delta n \approx \frac{\sigma_T^2 V_{bo}^{-1/3}}{3kT\eta^{2/3}}, \tag{13}$$

and from equation (9), the effective area of the low-SBH patch can be expressed as [25]

$$A_{eff} = \frac{8\pi\sigma_T^2}{9}\left(\frac{\eta}{V_{bo}}\right)^{1/3}. \tag{14}$$

The full line in figure 2 displays a fit of equation (9) to the experimental forward and reverse I–V data. The agreement between experimental data and fitted I–V curve in figure 2 is excellent, i.e., the experimental data are very well described by the thermionic emission theory of inhomogeneous Schottky contacts. The fitting parameters were $\Phi_{bo}^{hom} = 0.724$ eV, $R_s =$ 12 Ω, $\sigma_T = 2.26 \times 10^{-5}$ cm$^{2/3}$ V$^{1/3}$ (the standard deviation of patch parameter γ) and $\rho = 1.12 \times 10^{12}$ cm^{-2}, $N_d = 2.53 \times 10^{17}$ cm^{-3}, $A = 0.0143$ cm^2, $V_{bo} = 0.684$ eV and $T = 300$ K. From equations (12)–(14), $\Delta\Phi = 0.082$ eV, $\Delta n = 0.081$ (thus n =1.081) and $A_{eff} = 5.09 \times 10^{-13}$ cm^2 (thus patch radius = 4.062 nm) using the fitting parameters. This patch radius value is 15.45 times lower than the depletion layer width w. Leroy *et al* [21] have obtained a patch radius value for Au/n-GaAs SBDs that is 11.66 times lower than the depletion layer width. The value of $\Delta\Phi = 0.082$ eV from the fitting parameters is the same as the difference between the experimental I–V and C–V SBHs obtained for the Sn/n-GaAs SBD. The value of n = 1.081 from the fitting parameters is the same as the value of 1.081 obtained from the experimental I–V characteristics for the Sn/n-GaAs SBD by equation (6). Low patch radius value of 4.062 nm is because the substrate doping is high, N_d = 2.53×10^{17} cm^{-3}, and very low, $\sigma_T = 2.26 \times 10^{-5}$ cm$^{2/3}$ V$^{1/3}$, as can be seen from equation (14). $A_{eff} = 5.09 \times 10^{-13}$ cm^2 or patch radius = 4.062 nm obtained shows that the current through the low-barrier patches is dominant.

From the calculations we made using equation (9), we concluded that the current through the low-barrier patches is dominant and the current over the entire diode which has a uniform SBH of Φ_{bo}^{hom} and an area A is negligible. References [9, 26] indicate that the expression of the current flowing through the diode can be obtained by adding the current through the low-barrier patches to the current which passes through the surrounding homogeneous regions.

However, it is often reasonably assumed that the *I–V* characteristic is dominated by the current flow through the low-SBH patches. In fact, as pointed out by Ohdomari *et al* [40] even though the area covered by the low barrier represents only a few per cent fraction of the whole contact, the current through a contact is mainly affected by the presence of low-barrier regions. Therefore, [9] simultaneously fitted the experimental *I–V* curves at all the temperatures by using the contribution from the currents through inhomogeneous parts of the diode, $A_{\mathrm{eff}} = 2.46 \times 10^{-12}$ cm^2 in [9] and about 3×10^{-12} cm^2 for figure 7 at 300 K in [25].

As mentioned in [7–11, 13–17], the barrier height has a Gaussian distribution of the BHs over the Schottky contact area with the mean BH $\bar{\Phi}_{\mathrm{b}} = \Phi_{\mathrm{bo}}^{\mathrm{hom}}$ and the standard deviation of the barrier height distribution σ_{s}. The Gaussian distribution of the BHs yields the following expression for the BH [7–11, 13–17]:

$$\Phi_{\mathrm{eff}} = \Phi_{\mathrm{bo}}^{\mathrm{hom}} - \frac{q\sigma_{\mathrm{s}}^2}{2kT}. \tag{15}$$

The above expression for the apparent barrier height construction was already used by Song *et al* [14] and also by Werner and Gűttler [15]. The relation between the standard deviation of the apparent barrier height distribution σ_{s} and the standard deviation of the patch parameter γ is given by $\sigma_{\mathrm{s}} = \sigma_{\mathrm{T}}(V_{\mathrm{bo}}/\eta)^{1/3}$ from equations (12) and (15); thus, $\sigma_{\mathrm{s}} =$ 65.88 mV.

However, the fitting parameters such as $\Phi_{\mathrm{bo}}^{\mathrm{hom}} = 0.671$ eV, $\sigma_{\mathrm{T}} = 4.01 \times 10^{-5}$ cm$^{2/3}$ V$^{1/3}$ and $\rho = 5.91 \times 10^{7}$ cm^{-2} together with the other parameters above also gave a fit of equation (9) to the experimental forward *I–V* data of the Sn/n-GaAs SBD, but these fitting parameters do not give a fit to the reverse-bias branch. In such a case, the values of 0.257 eV, 0.251 and 1.56×10^{-12} cm^2 for $\Delta\Phi$, Δn and A_{eff} were obtained using the above fitting parameters, respectively; thus, $n = 1.251$. As can be seen, the value of $\Delta\Phi = 0.257$ eV from the fitting parameters is very larger than the difference between the experimental *I–V* and *C–V* SBH values obtained for the Sn/n-GaAs SBD. The value of $n = 1.251$ from these fitting parameters is very larger than the value of 1.081 obtained for the Sn/n-GaAs SBD from the experimental *I–V* characteristics by the standard procedure (equation (6)). Therefore, when the experimental data are described by the thermionic emission theory of inhomogeneous Schottky contacts, that is, while making a fit of equation (9) to the experimental *I–V* data, both the experimental forward and reverse *I–V* characteristics and the difference between the experimental *I–V* and *C–V* SBHs should be considered.

Let us look at whether or not the potential distribution near the interface of the inhomogeneous Sn/n-GaAs contact with $N_{\mathrm{d}} = 2.53 \times 10^{17}$ cm^{-3}, patch radius = 4.062 nm and $\Delta =$ 0.082 V is pinched off. As is well known, the conduction path in front of a small patch with a low SBH is pinched off if surrounded by high-SBH patches [25–29]. In such a case, the potential has a positive slope at small z values (depth from surface). The potential distribution of low-SBH circular patches is plotted for patches with different Δs in figure 4, using the above parameters in equation (6) of [25]. The critical Δ value for potential pinch-off for the Sn/n-GaAs SBD was calculated to be about 0.089 V using equation (7) of [25]. The larger Δ is, the greater is the degree of pinch-off. The

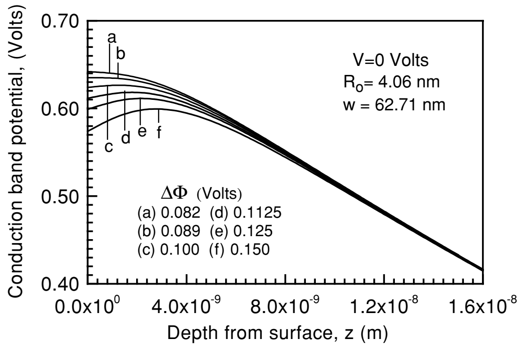

Figure 4. Diffusion potential for patches with different Schottky barrier height differences as a function of the distance z from the MS interface to the inside of the semiconductor.

experimental value of $\Delta = 0.082$ V obtained for the Sn/n-GaAs SBD is less than the critical value; therefore, there is no pinch-off effect, that is, the potential in front of the patch is not pinched off as can be seen from figure 4. Thus, the potential distribution approaches that of a uniform MS contact with the same SBH as that of the low-SBH patch. Furthermore, when the substrate doping is low, the low-SBH patch is more pinched off; when the substrate doping is high enough, the low-SBH patch is no longer pinched off [24, 25]. The critical doping value for an n-type GaAs MS contact with the patch radius = 4.062 nm, $\Phi_{\mathrm{bo}}^{\mathrm{hom}} = 0.724$ eV and $\Delta = 0.082$ V was calculated to be about $N_{\mathrm{d}} = 2.0 \times 10^{17}$ cm^{-3}. Therefore, the pinch-off effect was not observed for the inhomogeneous Sn/n-GaAs contact with $N_{\mathrm{d}} = 2.53 \times 10^{17}$ cm^{-3}. The numerically simulated potential distribution plot of the low-SBH patch for various n-type GaAs substrate doping levels is not shown here.

As mentioned above, a low patch radius value of 4.062 nm is due to the high level of substrate doping and very low standard deviation σ_{T} values. $A_{\mathrm{eff}} = 5.09 \times 10^{-13}$ cm^2 or patch radius = 4.062 nm obtained shows that the current through the low-barrier patches is dominant. Olbrich *et al* [12] demonstrated that BEEM measurements clearly reveal the pinch-off effect predicted by Tung and the pinch-off effect becomes less pronounced as the doping level and/or the patch dimension increases. They [12] deposited tiny Co metallization with extensions smaller than 4 nm leading to clusters of different sizes and densities for the formation of inhomogeneities on the $GaAs_{67}P_{33}$ surfaces ($N_{\mathrm{d}} = 5 \times 10^{16}$ cm^{-3}). They [12] have observed that the potential pinch-off effect plays a more significant role in the case of smaller Co patches. In our case, in spite of a low patch radius value of 4.062 nm, the pinch-off effect was not observed because the experimental value of $\Delta = 0.082$ V obtained for the Sn/n-GaAs SBD is less than the critical value and the substrate doping $N_{\mathrm{d}} = 2.53 \times 10^{17}$ cm^{-3} is higher than the critical value.

Figure 5 shows the simulated forward- and reverse-bias *I–V* characteristics using equation (9) for some representative parameters of our diode. To investigate the influence of the patch density on the transport properties, we varied the patch density ρ from 1.12×10^{9} cm^{-2} to 6.12×10^{12} cm^{-2} (thus 16 different patch density values), keeping the other parameters as used for the full line in figure 2 which displays a fit of

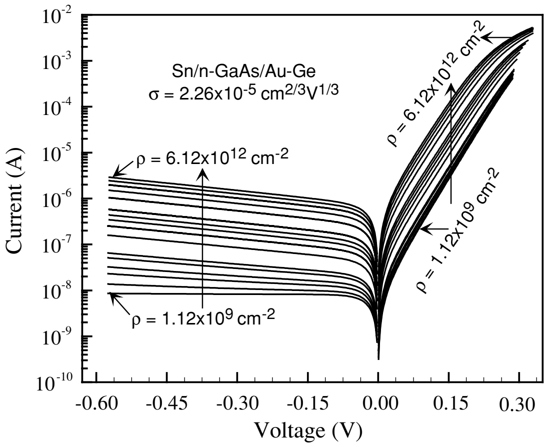

Figure 5. The forward- and reverse-bias *I–V* characteristics, calculated using equation (9), of an inhomogeneous n-GaAs Schottky barrier diode with $\Phi_{\rm bo}^{\rm hom} = 0.724$ eV, $R_s = 12\ \Omega$, $\sigma = 2.26 \times 10^{-5}$ cm$^{2/3}$ V$^{1/3}$, $N_d = 2.53 \times 10^{17}$ cm^{-3}, $A = 0.0143$ cm^2, $V_{\rm bo} = 0.684$ eV and $T = 300$ K. The patch density ρ was varied from 1.12×10^9 cm^{-2} to 6.12×10^{12} cm^{-2}. These values are 1.12×10^9, 1.12×10^{10}, 3.12×10^{10}, 5.12×10^{10}, 9.12×10^{10}, 1.12×10^{11}, 3.12×10^{11}, 5.12×10^{11}, 7.12×10^{11}, 9.12×10^{11}, 1.12×10^{12}, 2.12×10^{12}, 3.12×10^{12}, 4.12×10^{12}, 5.12×10^{12} and 6.12×10^{12} cm^{-2}.

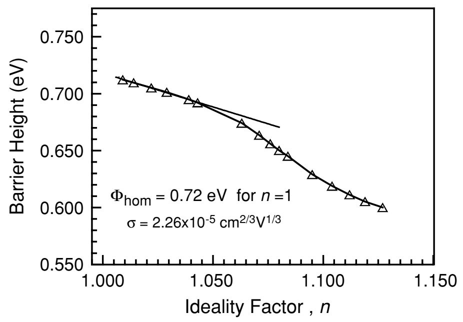

Figure 6. The effective barrier heights as a function of ideality factors determined from the forward bias *I–V* characteristics in figure 5 according to equations (5) and (6).

equation (9) to the experimental forward and reverse *I–V* data of the Sn/n-GaAs SBD. In our simulation, we made the simplifying assumption that all *I–V* characteristics in figure 5 are characterized by one and the same standard deviation of the patch parameter, $\sigma_T = 2.26 \times 10^{-5}$ cm$^{2/3}$ V$^{1/3}$. Whereas, the standard deviation of the patch parameter may vary from diode to diode. Then, the standard evaluation procedure was applied using equation (1) to the calculated *I–V* curves (figure 5) to obtain effective BHs and ideality factors. Thus, the correlation between the effective BHs and ideality factors [28–31, 35] obtained from the *I–V* characteristics in figure 5 is shown in figure 6. The $\Phi_b(n)$ curve is linear for ideality factors smaller than 1.05 and it is slightly bent above this value and approximately tends to linearity in the region of large ideality factors. Moreover, as can be seen from figure 5, the non-saturating behaviour of the reverse-bias curves decreases with decreasing patch density, and these curves approximately reach the saturation at the value of 1.12×10^9 cm^{-2}.

In conclusion, we have interpreted the experimental data by the well-known formula by Sullivan [24] and Tung [25, 26] for the total thermionic emission current including a patch function describing the inhomogeneities. It has been concluded that both the experimental forward and reverse *I–V* characteristics and the difference between the values of the experimental *I–V* and *C–V* SBHs should be considered when the thermionic emission theory of inhomogeneous Schottky contacts has been fitted to the experimental data, as in the full line in figure 2. An experimental BH difference of $\Delta = 0.082$ V has been obtained for the Sn/n-GaAs SBD that is less than the critical value; therefore, it has been seen that the potential in front of the patch is not pinched off.

References

[1] Tung R T 1993 *Contacts to Semiconductors* ed L J Brilson (New Jersey: Noyes)
[2] Biber M, Gullu O, Forment S, Van Meirhaeghe R L and Turut A 2006 *Semicond. Sci. Technol.* **21** 1
[3] John A and Palaniappan S 2005 *Polymer* **46** 12037
[4] Horvath Zs J, Bosacchi A, Franchi S, Gombia E, Mosca R and Motta A 1994 *Mater. Sci. Eng.* B **28** 429
[5] Huang S H, Tian Y and Lu F 2004 *Appl. Surf. Sci.* **234** 362
[6] Kanbur H, Altindal S and Tataroglu A 2005 *Appl. Surf. Sci.* **252** 1732
[7] von Wenckstern H, Biehne G, Rahman R A, Hochmuth H, Lorenz M and Grundmann M 2006 *Appl. Phys. Lett.* **88** 092102
[8] Sehgal B K, Balakrishnan V R, Gulati R and Tewari S P 2003 *J. Semicond. Technol. Sci.* **3** 1–12
[9] Roccaforte F, La Via F, Raineri V, Pierobon R and Zanoni E 2003 *J. Appl. Phys.* **93** 9137
[10] Pérez R, Mestres N, Montserrat J, Tournier D and Godignon P 2005 *Phys. Status Solidi* a **202** 692
[11] Cetin H and Ayyildiz E 2005 *Semicond. Sci. Technol.* **20** 625
[12] Olbrich A, Vancea J, Kreupl F and Hoffmann H 1997 *Appl. Phys. Lett.* **70** 2559
Olbrich A, Vancea J, Kreupl F and Hoffmann H 1998 *J. Appl. Phys.* **83** 358
[13] Özdemir A F, Türüt A and Kökçe A 2006 *Semicond. Sci. Technol.* **21** 298
[14] Song Y P, Van Meirhaeghe R L, Lafléré W H and Cardon F 1986 *Solid-State Electron.* **29** 633
[15] Werner J H and Güttler H H 1991 *J. Appl. Phys.* **69** 1522
[16] Chand S and Kumar J 1995 *Semicond. Sci. Technol.* **10** 1680
Chand S and Bala S 2005 *Appl. Surf. Sci.* **252** 358
[17] Chand S and Kumar J 1996 *Semicond. Sci. Technol.* **11** 1203
Chand S and Kumar J 1997 *Appl. Phys.* A **65** 171
[18] Karataş Ş, Altındal Ş, Türüt A and Özmen A 2003 *Appl. Surf. Sci.* **217** 250
[19] Osvald J 1999 *J. Appl. Phys.* **85** 1935
Dobrocka E and Osvald J 1994 *Appl. Phys. Lett.* **65** 575
Osvald J 2006 *Solid-State Electron.* **50** 228
[20] Anand S, Carlsson S B, Deppert K, Montelius L and Samuelson L 1996 *J. Vac. Sci. Technol.* B **14** 2794
[21] Vanalme G M, Goubert L, Van Meirhaeghe R L, Cardon F and van Meirhaeghe P 1999 *Semicond. Sci. Technol.* **14** 871
Vanalme G M, Van Meirhaeghe R L, Cardon F and van Daele P 1997 *Semicond. Sci. Technol.* **12** 907
Leroy W P, Opsomer K, Forment S and Van Meirhaeghe R L 2005 *Solid-State Electron.* **49** 878
[22] Im H J, Ding Y, Pelz J P and Choyke W J 2001 *Phys. Rev.* B **64** 075310
[23] Kampen T U and Mönch W 1995 *Surf. Sci.* **331–333** 490
[24] Sullivan J P, Tung R T, Pinto M R and Graham W R 1991 *J. Appl. Phys.* **70** 7403
[25] Tung R T 1992 *Phys. Rev.* B **45** 13509
[26] Tung R T 2001 *Mater. Sci. Eng.* R **35** 1–138

[27] Rossi R C, Tan M X and Lewis N S 2000 *Appl. Phys. Lett.* **77** 2698
Rossi R C and Lewis N S 2001 *J. Phys. Chem.* B **105** 12303
[28] Schmitsdorf R F, Kampen T U and Mönch W 1997 *J. Vac. Sci. Technol.* B **15** 1221
[29] Jones F E, Wood B P, Myers J A, Daniels C H and Lonergan M C 1999 *J. Appl. Phys.* **86** 6431
Jones F E and Lonergan M C 2001 *J. Chem. Phys.* **115** 433
[30] Gümüş A, Türüt A and Yalçın N 2002 *J. Appl. Phys.* **91** 245
[31] Akkılıc K, Aydın M E and Turut A 2004 *Phys. Scr.* **70** 364
[32] Türüt A, Batı B, Kökçe A, Sağlam M and Yalçın N 1996 *Phys. Scr.* **53** 118
[33] Rhoderick E H and Williams R H 1988 *Metal–Semiconductor Contacts* 2nd edn (Oxford: Clarendon)
[34] Van der Ziel A 1968 *Solid State Physical Electronics* 2nd edn (Englewood Cliffs, NJ: Prentice-Hall)
[35] Mönch W 1995 *Semiconductor Surfaces and Interfaces* 2nd edn (Berlin: Springer)
[36] Newman N, van Schilfgaarde M, Kandelwicz T, Williams M D and Spicer W E 1986 *Phys. Rev.* B **33** 1146
[37] Paoli T L and Barnes P A 1976 *Appl. Phys. Lett.* **28** 714
[38] Cheung S K and Cheung N W 1986 *Appl. Phys. Lett.* **49** 85
[39] Werner J H 1988 *Appl. Phys.* A **47** 291
[40] Ohdomari I, Kuan T S and Tu K N 1979 *J. Appl. Phys.* **50** 7020